Université de Montréal

Brisure de la symétrie icosaédrique du C_{60} vers des fullerènes plus grands et les nanotubes apparentés

par

Emmanuel Bourret

Département de physique
Faculté des arts et des sciences

Mémoire présenté à la Faculté des études supérieures
en vue de l'obtention du grade de
Maître ès sciences (M.Sc.)
en Physique

19 mars 2018

Sommaire

La symétrie icosaédrique exacte du fullerène C_{60} est vue comme une orbite du groupe de Coxeter H_3. Cette orbite est décomposable en orbites des sous-groupes symétriques de rangs inférieurs. Les orbites forment un empilement de couches parallèles centrées sur un axe traversant le C_{60} de part en part. En insérant au milieu de l'empilement un certain nombre d'orbites du sous-groupe étudié, on peut retrouver la structure d'un fullerène plus grand. En répétant l'insertion, on peut obtenir des fullerènes et nanotubes de toute longueur souhaitable. Ce mémoire présente les cas où les sous-groupes utilisés sont notés A_2 et $A_1 \times A_1$, car ils sont respectivement isomorphes aux groupes de Weyl des algèbres de Lie simples A_2 et $A_1 \times A_1$. Ces deux cas permettent d'obtenir à terme des nanotubes de type zigzag et chiral. Des avenues de généralisation de la méthode sont discutées dans la dernière partie de ce mémoire.

Mots-clés : fullerènes, nanotubes, symétrie icosaédrique, brisure de symétrie, polytopes

Summary

Exact icosahedral symmetry of C_{60} fullerene is viewed as an orbit of H_3 Coxeter group. This orbit is decomposable into orbits of symmetrical subgroups of lower ranks. The orbits form a stack of parallel layers centered on an axis traversing the C_{60} from side to side. By inserting in the middle of the stack a certain number of orbits of the studied subgroup, one can find the structure of a larger fullerene. By repeating the insertion, fullerenes and nanotubes of any desirable length can be obtained. This thesis presents the cases where the subgroups used are denoted A_2 and $A_1 \times A_1$, since they are respectively isomorphic to the Weyl groups of simple Lie algebras A_2 and $A_1 \times A_1$. These two cases make it possible eventually to obtain nanotubes of the zig-zag and chiral type. Avenues of generalization of the method are discussed in the last part of this thesis.

Keywords : fullerenes, nanotubes, icosahedral symmetry, symmetry breaking, polytopes

Table des matières

Table des figures

Dédicaces

À Sally et Olivia le petit monstre,

Remerciements

J'aimerais d'abord remercier Jiri Patera, mon directeur de recherche à l'Université de Montréal et Elisa Shahbazian, ma codirectrice de recherche chez Ooda Technologies. Je tiens à remercier particulièrement Jiri Patera pour la variété de problèmes intéressants qu'il m'a soumis et la grande liberté avec laquelle il m'a laissé les étudier.

J'aimerais aussi remercier mes collègues Maria Myronova, Zofia Grabowiecka et Marzena Szajewska pour leur aide tout au long de nos collaborations et les discussions intéressantes qui en découlèrent.

Je remercie également les membres du Bleach Club, buvez-en un à ma santé.

Je tiens à remercier particulièrement Christina Gagnon et Elyse Robin-Boulanger qui m'ont supporté en me bottant le derrière à chaque fois où je ne travaillais pas suffisamment à leur goût (soit toujours). Un gros merci les filles.

Enfin, je tiens à remercier mes parents, famille et amis qui m'ont soutenu dans mes efforts tout au long de mes études, ainsi que pour leur aide et leurs encouragements.

Introduction

La classification des problèmes physiques en fonction de leurs symétries est une approche qui s'est avérée fructueuse dans la description de systèmes observés dans la nature. Parmi ces systèmes, les structures discrètes dérivées des symétries des groupes de réflexions finis, telles que les nanostructures de carbone, sont encore à ce jour largement inexplorées. L'intérêt de ces structures vient principalement de la découverte de leurs étonnantes propriétés qui mena à leur étude intensive au cours des dernières années. En raison de leurs exceptionnelles propriétés physiques, chimiques et mécaniques, une variété croissante d'applications fut trouvée [15, 24, 25, 26, 32]. Bien que les nanomatériaux les plus prometteurs soient les graphènes, les fullerènes et les nanotubes de carbone, leur structure géométrique est encore à ce jour peu étudiée. Une façon moderne d'obtenir ces structures est l'utilisation des groupes de réflexions finis, aussi appelés groupes de Coxeter.

La classification des groupes de Coxeter finis est un accomplissement majeur du début du XX$^{\text{e}}$ siècle. Il y a deux types de groupes de réflexions finis, les groupes cristallographiques, aussi appelés groupes de Weyl, et les groupes non cristallographiques. Les groupes de Weyl sont intimement liés aux l'algèbres de Lie simples et très souvent dénotées dans la littérature par les symboles de celles-ci [6, 17]. Plus précisément, $A_n, n = 1, \ldots, < \infty$, $B_n, n = 2, \ldots, < \infty$, $C_n, n = 3, \ldots, < \infty$, $D_n, n = 4, \ldots, < \infty$ et les cinq groupes exceptionnels, nommés E_6, E_7, E_8, F_4 et G_2. Plusieurs isomorphismes bien connus complètent cette notation, soit $C_2 \cong B_2$, $D_2 \cong A_1 \times A_1$ et $D_3 \cong A_3$.

Cependant, il existe également des groupes non cristallographiques qui, dans ce travail, nous intéressent. Il y a trois groupes de ce type, soit H_2, H_3 et H_4, qui sont respectivement de dimension 2, 3 et 4 [10, 23]. En général, en deux dimensions il y a une infinité de ces groupes rassemblés sous la notation $I_2(p)$, pour p un entier et $p \neq 3{,}4{,}6$ (afin d'exclure les trois cas déjà compris dans les groupes de Weyl), mais seul le cas $p = 5$ est pertinent à notre étude. En dimension 3 ainsi qu'en dimension 4, il n'y a qu'un seul groupe de type non cristallographique. Dans ce travail, nous nous intéressons plus particulièrement au groupe H_3 qui correspond au groupe des symétries d'un fullerène C_{60}, soit la symétrie icosaédrique. Notre objectif est de définir sa décomposition en sous-groupes de rangs inférieurs, car une fois cette décomposition connue, il est possible de définir comment briser la symétrie du C_{60}.

De cette façon, nous obtenons une description de la structure du fullerène C_{60} comme un empilement de couches, appelée « stack of pancakes », qui joue un rôle crucial dans notre travail. Briser le fullerène en deux nous permet de construire pas à pas des fullerènes plus grands et les trois types de nanotubes connus, soit chaise (armchair), zigzag et chiral.

En général, il est pratique d'identifier les groupes de réflexions finis par leur diagramme de Coxeter-Dynkin, par exemple, le diagramme du groupe H_3 représenté à la Figure 1.1 [18]. Les noeuds des diagrammes, représentant les vecteurs de base dans l'espace euclidien réel de n-dimensions, sont appelés racines simples de l'algèbre de Lie correspondante. Leur rôle dans les groupes de réflexions finis peut être compris comme les vecteurs normaux des plans de réflexions, en assumant que les plans de réflexions ont comme point commun l'origine.

Un des principaux outils de ce travail est l'ensemble des orbites des groupes de réflexions. En effet, il est possible de voir le fullerène C_{60} comme une des orbites du groupe de Coxeter H_3, et donc de le décomposer en orbites des sous-groupes de rangs inférieurs. Il y a trois sous-groupes d'intérêt pour H_3, soit H_2, A_2 et $A_1 \times A_1$. Parmi ces sous-groupes, le travail actuel portera sur les deux derniers cas, car le cas du sous-groupe H_2 est traité en profondeur par Bodner et al. [2, 4]. Brièvement, ces articles présentèrent la méthode utilisée dans ce travail afin de construire, à partir du fullerène C_{60}, les fullerènes C_{70}, C_{80}, et ainsi de suite jusqu'à un nanotube de type chaise.

Deux chapitres composent ce mémoire. Le premier explore le cas où la symétrie du C_{60} est brisée par l'ajout d'orbites du sous-groupe A_2 jusqu'à l'obtention d'un nanotube de type zigzag. Le deuxième chapitre se concentre sur le cas où la symétrie est brisée selon le sous-groupe $A_1 \times A_1$. Cette avenue permet d'obtenir à terme un nanotube de type chiral. Dans la dernière partie de ce travail, des avenues sont discutées afin de généraliser la méthode, de construire des nanotubes de différents diamètres, et aussi de l'appliquer sur d'autres structures similaires à celle du fullerène C_{60}.

Chapitre 1

Icosahedral symmetry breaking : C_{60} to C_{78}, C_{96} and to related nanotubes

Cet article a été publié dans la revue *Acta Crystallographica Section A : Foundations and Advances* [voir 3].

Les principales contributions de *Emmanuel Bourret* à cet article sont présentées.

— réalisation des calculs numériques générant les fullerènes ;

— vérification que la brisure de symétrie proposée était bien la minimale en vérifiant toutes les possibilités ;

— aide à la rédaction de l'article ainsi qu'au processus de révision et de correction.

Icosahedral symmetry breaking : C_{60} to C_{78}, C_{96} and to related nanotubes

Mark Bodner
MIND Research Institute,
111 Academy Drive,
Irvine, CA, USA 92617

Emmanuel Bourret
Centre de recherches mathématiques,
Université de Montréal,
C.P. 6128, Succursale A,
Montréal, Canada H3C 3J7

Jiri Patera
Centre de recherches mathématiques,
Université de Montréal,
C.P. 6128, Succursale A,
Montréal, Canada H3C 3J7

Marzena Szajewska
Institute of Mathematics,
University of Bialystok,
Akademicka 2,
Bialystok, Poland PL-15-267

Résumé

La symétrie icosaédrique exacte du C_{60} est vue comme l'union de 12 orbites du sous-groupe symétrique d'ordre 6 du groupe icosaédrique d'ordre 120. Ici, ce sous-groupe est noté par A_2, car il est isomorphe au groupe de Weyl de l'algèbre de Lie simple A_2. Huit des orbites de A_2 sont des hexagones et quatre sont des triangles. Seulement deux des hexagones apparaissent comme faisant partie de la surface de la coquille du C_{60}. Les orbites forment un empilement de couches parallèles centrés sur l'axe du C_{60} passant par les centres de deux hexagones opposés à la surface du C_{60}. En insérant au milieu de l'empilement deux orbites de A_2 de six points chaque et deux orbites de A_2 de trois points chaque, on peut retrouver la structure du C_{78}. En répétant l'insertion, on obtient le C_{96} ; plusieur insertions de ce genre génèrent des nanotubes de toute longueur souhaitable. Cinq polytopes différents avec 78 sommets similaires au carbone sont décrits ; seulement deux d'entre eux peuvent être augmentés aux nanotubes.

Mots-clés : groupe de Coxeter fini, brisure de symétrie, fullerènes, nanotubes

Abstract

Exact icosahedral symmetry of C_{60} is viewed as the union of 12 orbits of the symmetric subgroup of order 6 of the icosahedral group of order 120. Here, this subgroup is denoted by A_2, because it is isomorphic to the Weyl group of the simple Lie algebra A_2. Eight of the A_2 orbits are hexagons and four are triangles. Only two of the hexagons appear as part of the C_{60} surface shell. The orbits form a stack of parallel layers centered on the axis of C_{60} passing through the centers of two opposite hexagons on the surface of C_{60}. By inserting into the middle of the stack two A_2 orbits of six points each and two A_2 orbits of three points each, one can match the structure of C_{78}. Repeating the insertion, one gets C_{96}; multiple such insertions generate nanotubes of any desirable length. Five different polytopes with 78 carbon-like vertices are described; only two of them can be augmented to nanotubes.

Keywords: finite Coxeter group, symmetry breaking, fullerenes, nanotubes

1.1. Introduction

The present paper is an independent continuation of the work reported by Bodner et al. [2], where the icosahedral symmetry of the fullerene C_{60} was broken to the subgroup H_2 of the icosahedral group H_3, providing a mechanism for the generation of larger fullerenes of the form C_{60+N10}. The subject of our study here is icosahedral symmetry breaking to the subgroup A_2, more precisely to the Weyl group of the simple Lie algebra A_2, which is the finite symmetry group of order 6 isomorphic to the symmetric group of three elements.

While Bodner et al. [2] reported the fullerene polytopes related to C_{60} were C_{70}, C_{80}, C_{90}, and related nanotubes, in this paper the fullerenes arising from C_{60} are C_{78}, C_{96}, C_{114}, and

other related types of nanotubes. In general, the situation here is more complicated than reported by Bodner et al. [2], as there are five different fullerene C_{78} polytopes. Two of them are the results of two variants of the symmetry breaking $H_3 \to A_2$, each of them leading to a series of larger fullerenes and nanotubes (Dresselhaus et al. [11]; Harris [16]; Cataldo et al. [7]).The remaining three C_{78} polytopes have no detectable subgroup symmetry and no related nanotubes.

The five types of C_{78} polytopes, $C_{78}(I)$, $C_{78}(II)$, ..., $C_{78}(V)$ [1], are distinguished by the pairs of the nearest pentagons on their surface 'central belt', *i.e.* the three rings of hexagons and pentagons in the middle of the polytope oriented along the α_3 direction. While $C_{78}(I)$ and $C_{78}(II)$ can be extended to larger polytopes and to nanotubes of any desired length by insertion of a corresponding number of additional rings of nine hexagons into the middle of the structure, the polytopes $C_{78}(III)$, $C_{78}(IV)$ and $C_{78}(V)$ cannot be further extended further in any systematic way.

In this paper, we continue to pursue the general idea of symmetry breaking, or symmetry reduction, as is often done in science [27] as a mechanism for the generation of specific large fullerenes existing in nature (Balasubramanian [1]; Wang et al. [31]; Fowler and Manolopoulos [13]; Lin et al. [21, 22]; Zhang et al. [33]). Large symmetry, say G, is broken or reduced to the symmetry of one of the subgroups, say $G' \subset G$. Here the symmetry group G is the icosahedral group (denoted H_3) of order 120, acting in the three-dimensional real Euclidean space $\mathbb{R}^3$.

Here we explore one of the three 'natural' avenues of breaking H_3 symmetry. The group H_3 is generated by three reflection operations called here r_1, r_2, and r_3 (for an elaboration on these reflections see subsection 1.2.2). There are three ways of breaking H_3 to retain only two of the three reflections as generating elements for the subgroup $G' \subset H_3$. Specifically we have the following possibilities for G'

$$r_2, r_3 \quad \text{generate} \quad G' = H_2 \quad |H_2| = 10 \tag{1.1}$$

$$r_1, r_2 \quad \text{generate} \quad G' = A_2 \quad |A_2| = 6 \tag{1.2}$$

$$r_1, r_3 \quad \text{generate} \quad G' = A_1 \times A_1 \quad |A_1 \times A_1| = 4, \tag{1.3}$$

where we have introduced notation for the three types of the subgroups G' and show the order $|G'|$ of G'. The three ways of symmetry breaking we mentioned above, do not exhaust all possible symmetry breakings of H_3, however they appear more naturally or less arbitrary having no built-in parameters to fix.

The case (1.1) was studied by Bodner et al. [2, 4], which led from C_{60} to the generation of the fullerenes C_{70}, C_{80}, C_{90},... and to corresponding nanotubes.

1. For clarity, we specify here the point groups of the C_{78} isomers. In the Schönflies convention, $C_{78}(I)$ and $C_{78}(II)$ are D_{3h}, $C_{78}(III)$ is D_3 and, $C_{78}(IV)$ and $C_{78}(V)$ are C_{2v}. These are given in paper by Fowler and Manolopoulos [13].

The case (1.2) is the subject of the present paper.

The case (1.3) was not studied as a symmetry-breaking problem. It will be considered elsewhere.

If the icosahedral symmetry breaking is guided by the subgroup A_2, the polytope with broken symmetry closest to C_{60} is the fullerene C_{78}. It turns out that there are two possible versions of the symmetry-breaking mechanism, leading to two different C_{78} polytopes. Both versions can be extended by breaking the symmetry an arbitrary number of times, leading to the generation of nanotubes of any desired length. However five different C_{78} molecules have been identified theoretically, with the two considered here being among them. All are near spherical shells with surfaces built by hexagons and pentagons [see, for example, Table A in the book by Fowler and Manolopoulos [13]]. In the cases of the three additional C_{78} polytopes, one finds no large subgroup of the icosahedral group, whose symmetry would be retained during the symmetry breaking.

In addition to the fullerene C_{60}, defined by its dominant point $\omega_1 + \omega_2$, there are two other polytopes with exact icosahedral symmetry and 60 vertices. We do not call those polytopes fullerenes. Their dominant points are $\omega_2 + \omega_3$ and $\omega_1 + \omega_3$. The two cases are easily distinguished from the fullerene C_{60} by their 2-faces (Champagne et al. [9]). In the one case these faces are decagons and triangles, while in the second case the 2-faces are pentagons, squares, and triangles, while the C_{60} fullerene is built from pentagons and hexagons. The general method of identification and description of faces of n-dimensional polytopes was found by Champagne et al. [9]. For an extensive application of the method see Szajewska [30].

It was shown in the paper by Bodner et al. [2] that there exists a continuum of different polytopes that display an exact icosahedral symmetry and have 60 vertices. They are called the 'twisted fullerenes'. Their shell is formed by 12 regular pentagons and 20 non-regular hexagons which have three sides of one length and three sides of another length. It appears that none of these C_{60} stereoisomers allow extension to nanotubes.

1.2. The fullerene C_{60}

The three reflections in mirrors that have a common point at the origin of the three-dimensional Euclidean space $\mathbb{R}^3$ generate reflection groups in $\mathbb{R}^3$. Relative angles of the mirrors determine whether the group is finite or not and which group it is. The angles between the mirrors are specified by the relative angles of the three normal vectors to the mirrors, α_1, α_2, α_3. Fixing for convenience the length of the three α-vectors to be the same, then the angles are read from the Coxeter diagram (see Fig. 1.1),

one has the α-basis of the icosahedral symmetry in $\mathbb{R}^3$. The α-basis $\{\alpha_1,\alpha_2,\alpha_3\}$ of vector normals to the reflection mirrors define the icosahedral group.

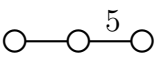

Figure 1.1. Coxeter diagram of H_3. Its nodes are taken to stand for the basis vectors of α-basis, numbered from left to right. Connecting lines specify the angles between basis vectors: a single line without the number means that the angle is 120°, a line with the number 5 means 144°, and the absence of a direct connection implies orthogonality of the two basis vectors. It is also sometimes useful to read the nodes of the diagram as the vectors of the ω-basis, or for the reflections r_1, r_2, r_3 in mirrors orthogonal to vectors of the α-basis and intersecting at the origin of $\mathbb{R}^3$.

The α-basis is defined by the matrix C of the scalar products of the basis vectors,

$$C = (C_{jk}) = (\langle \alpha_j, \alpha_k \rangle) = \begin{pmatrix} 2 & -1 & 0 \\ -1 & 2 & -\tau \\ 0 & -\tau & 2 \end{pmatrix}, \qquad \tau = \tfrac{1}{2}\left[1 + (5)^{1/2}\right] = 2\cos \pi/5\,. \tag{1.4}$$

1.2.1. Icosahedral bases in $\mathbb{R}^3$

A considerable simplification of the description of the polytopes with icosahedral symmetry can be achieved when bases defined by the symmetry group are used, since the bases are not orthogonal.

Besides the α-basis we use the ω-basis that is reciprocal, or equivalently, dual to the α-basis. It is defined by the requirement

$$\langle \alpha_j, \omega_k \rangle = \delta_{jk}\,, \quad j,k = 1,2,3\,. \tag{1.5}$$

It is given by the matrix C^{-1}, inverse to C. Matrix elements of C^{-1} are the scalar products of the vectors of the ω-basis (Champagne et al. [9]).

$$(C^{-1}_{jk}) = (\langle \omega_j, \omega_k \rangle) = \frac{1}{2} \begin{pmatrix} 2+\tau & 2+2\tau & 1+2\tau \\ 2+2\tau & 4+4\tau & 2+4\tau \\ 1+2\tau & 2+4\tau & 3+3\tau \end{pmatrix} \tag{1.6}$$

Of practical importance are the relations:

$$\alpha_j = \sum_{k=1}^{3} C_{jk}\omega_k\,, \quad \omega_k = \sum_{j=1}^{3} C^{-1}_{kj}\alpha_j\,. \tag{1.7}$$

It should be noted that requirement (1.5) does not imply that α_k and ω_k are collinear for any $k = 1,2$, or 3. Indeed, the vectors ω_k are of different length (1.6). In particular,

$$\begin{aligned} \omega_1 &= \tfrac{1}{2}(2+\tau)\alpha_1 + (1+\tau)\alpha_2 + \tfrac{1}{2}(1+2\tau)\alpha_3 \\ \omega_2 &= (1+\tau)\alpha_1 + (2+2\tau)\alpha_2 + (1+2\tau)\alpha_3 \\ \omega_3 &= \tfrac{1}{2}(1+2\tau)\alpha_1 + (1+2\tau)\alpha_2 + \tfrac{3}{2}(1+\tau)\alpha_3 \end{aligned} \tag{1.8}$$

Of interest to us here is the subgroup A_2 of H_3. It is the dihedral group of order 6, and it is isomorphic to the symmetric group of three elements. It is conveniently fixed inside H_3

by choosing α_1 and α_2 to be its α-basis, *i.e.* vectors normal to the refection mirrors of A_2. As the dual basis we choose ω_1 and ω_2 because they satisfy requirement (1.5) for $j,k = 1,2$. Note that by requirement (1.5), the direction orthogonal to the plane spanned by ω_1 and ω_2 is the direction of α_3.

1.2.2. Icosahedral reflections

A reflection is called icosahedral provided it is a reflection in one of the three mirrors whose orientation is fixed by the vector normals α_1, α_2, α_3. We denote by r_1, r_2, and r_3 the corresponding reflection operations. Any point $x \in \mathbb{R}^3$ is reflected according to

$$r_k x = x - \langle x,\alpha_k\rangle \alpha_k, \qquad k = 1,2,3, \qquad x \in \mathbb{R}^3. \tag{1.9}$$

In particular, $r_k\alpha_j = \alpha_j - \langle \alpha_k,\alpha_j\rangle \alpha_k$ and also $r_k\omega_j = \omega_j - \delta_{jk}\alpha_k$. By explicit calculation one can check the following identities:

$$r_1^2 = r_2^2 = r_3^2 = 1, \qquad (r_1 r_2)^3 = 1, \qquad (r_1 r_3)^2 = 1, \qquad (r_2 r_3)^5 = 1, \tag{1.10}$$

where 1 stands for an identity operation.

Repeated application of the reflection operations (1.9) to any point x generate precisely one orbit of the H_3 group. Any point x cannot belong to two orbits of H_3. The number of distinct points in any orbit is easily found, provided x is given relative to the ω-basis (Champagne et al. [9]). As usual, we interpret the points of the orbit as vertices of an icosahedral polytope in $\mathbb{R}^3$. The orbit of 60 elements/vertices arises when $x = a\omega_1 + b\omega_2$ with $a,b > 0$. If in addition, we have $a = b$, the polytope is the fullerene C_{60}. If $a \neq b$, one gets the 'twisted' polytope of the paper by Bodner et al. [4], still displaying exact icosahedral symmetry, but whose edges between hexagons are of different length than the edges separating hexagons and pentagons.

The faces of C_{60} have been described previously (Champagne et al. [9]; Bodner et al. [2, 4]) together with a method for finding them. There are 60 faces of dimension 0 (vertices), 20 hexagonal faces and 12 pentagonal ones (faces of dimension 2), and 30 edges between two hexagons and 60 edges separating hexagons and pentagons (faces of dimension 1).

1.3. The A_2 orbits of vertices of C_{60}

The vertices of C_{60} are generated by the reflections (1.9) from any of its points, although it is practical to identify an orbit by its unique dominant point, the only orbit point that has non-negative coordinates in the ω-basis. Therefore the 60 points belong to a single orbit of vertices of the icosahedral group H_3. All 60 vertices of the polytope are listed in the ω-basis of H_3 by Bodner et al. [2, 4]. However, when one looks at the same set of 60 vertices

from the perspective of a subgroup of H_3, in the present case the subgroup A_2, the vertices decompose into several orbits of A_2.

Here the list of 60 vertices of C_{60} is reproduced from Bodner et al. [2, 4].

$\boxed{\pm(1,1,0)}$	$\pm(-1,2,0)$	$\pm(2,-1,\tau)$	$\pm(1,-2,2\tau)$	$\pm(\tau,-2-\tau,1+2\tau)$
$\boxed{\pm(-1,-1,2\tau)}$	$\pm(-2,2+\tau,-\tau)$	$\pm(2+\tau,-\tau,1)$	$\boxed{\pm(1,2\tau,-2\tau)}$	$\pm(-1,1+2\tau,-2\tau)$
$\pm(-2,1,\tau)$	$\pm(-2-\tau,2,1)$	$\boxed{\pm(2+\tau,0,-1)}$	$\pm(1+2\tau,-2\tau,2)$	$\pm(2\tau,-1-2\tau,2+\tau)$
$\boxed{\pm(1+2\tau,0,-2)}$	$\boxed{\pm(\tau,2\tau,-1-2\tau)}$	$\pm(-2-\tau,2+\tau,-1)$	$\pm(-1-2\tau,1,2)$	$\boxed{\pm(-\tau,-2,1+2\tau)}$
$\boxed{\pm(0,-2-\tau,3\tau)}$	$\boxed{\pm(2\tau,\tau,-2-\tau)}$	$\pm(-\tau,3\tau,-1-2\tau)$	$\pm(3\tau,-2\tau,1)$	$\boxed{\pm(-2\tau,-1,2+\tau)}$
$\boxed{\pm(2,\tau,-\tau)}$	$\pm(3\tau,-\tau,-1)$	$\pm(-2\tau,3\tau,-2-\tau)$	$\boxed{\pm(0,1+2\tau,-3\tau)}$	$\pm(-1-2\tau,1+2\tau,-2)$

The points that are in boxes specify the orbits of the subgroup A_2 of H_3. They are distinguished by the signs of their first and second coodinates. These signs coincide. Therefore, the points taken with the non-negative signs of the first two coordinates are the highest ('dominant') points on the orbit. When both coordinates are positive, its A_2 orbit has six points. When one of the coordinates is zero, its orbit consists of three points. There are eight orbits of six points and four orbits of three points.

Example 1.1. *During the transformation of a vector given relative to the basis* $\{\omega_1,\omega_2,\omega_3\}$ *to the basis* $\{\omega_1,\omega_2,\alpha_3\}$*, dominant vectors remain dominant in their orbits, because the transformation leave the first two coordinates unchanged.*

Suppose (a,b,c) *is given relative to the basis* $\{\omega_1,\omega_2,\omega_3\}$*. In order to transform it to the basis* $\{\omega_1,\omega_2,\alpha_3\}$*, one proceeds as follows,*

$$(a,b,c)\begin{pmatrix}1 & 0 & \frac{1}{2}+\tau\\ 0 & 1 & 1+2\tau\\ 0 & 0 & \frac{3}{2}+\frac{3}{2}\tau\end{pmatrix} = (a,b,a(\tfrac{1}{2}+\tau)+b(1+2\tau)+c(\tfrac{3}{2}+\tfrac{3}{2}\tau))$$
$$= (a,b,\tfrac{1}{2}(a+2b+3c)+\tau\tfrac{1}{2}(2a+4b+3c))\,.$$

Thus one gets the following specific transformations:
$(1,1,0)\longrightarrow(1,1,\frac{3}{2}+3\tau)$, $(2,\tau,-\tau)\longrightarrow(2,\tau,\frac{3}{2}+2\tau),\ldots$

$\boxtimes$

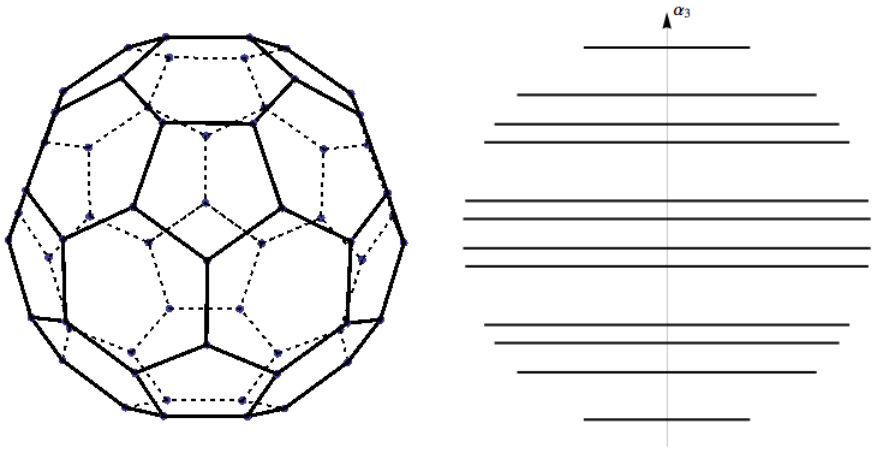

Figure 1.2. The polytope C_{60} viewed from the direction parallel to the plane spanned by ω_1 and ω_2. The orbits of A_2 appear as horizontal segments ('stack of pancakes').

Rewriting the vertices of C_{60} in the A_2 basis, i.e. $\{\omega_1, \omega_2, \alpha_3\}$, we have:

$$
\begin{array}{lllll}
\boxed{\pm(1,1,\tfrac{3}{2}+3\tau)} & \pm(-\tau,3\tau,\tfrac{1}{2}) & \boxed{\pm(-1,-1,\tfrac{3}{2}+3\tau)} & \pm(2,-1,\tfrac{3}{2}+3\tau) & \pm(-2-\tau,2+\tau,\tfrac{1}{2}+2\tau) \\
\pm(1,-2,\tfrac{3}{2}+3\tau) & \pm(-3\tau,\tau,\tfrac{1}{2}) & \pm(2+\tau,-\tau,\tfrac{3}{2}+2\tau) & \pm(\tau,-2-\tau,\tfrac{3}{2}+2\tau) & \boxed{\pm(0,-1-2\tau,-\tfrac{1}{2}+\tau)} \\
\boxed{\pm(1,2\tau,\tfrac{3}{2}+\tau)} & \pm(3\tau,-2\tau,\tfrac{1}{2}) & \boxed{\pm(2+\tau,0,\tfrac{1}{2}+2\tau)} & \pm(1+2\tau,-2\tau,\tfrac{3}{2}+\tau) & \pm(2\tau,-1-2\tau,\tfrac{3}{2}+\tau) \\
\pm(-2,1,\tfrac{3}{2}+3\tau) & \boxed{\pm(\tau,2\tau,\tfrac{1}{2})} & \boxed{\pm(-\tau,-2,\tfrac{3}{2}+2\tau)} & \pm(-1-2\tau,1,\tfrac{3}{2}+\tau) & \boxed{\pm(1+2\tau,0,-\tfrac{1}{2}+\tau)} \\
\pm(-1,2,\tfrac{3}{2}+3\tau) & \boxed{\pm(-2\tau,-\tau,\tfrac{1}{2})} & \boxed{\pm(-2\tau,-1,\tfrac{3}{2}+\tau)} & \pm(-2-\tau,2,\tfrac{3}{2}+2\tau) & \boxed{\pm(0,-2-\tau,\tfrac{1}{2}+2\tau)} \\
\boxed{\pm(2,\tau,\tfrac{3}{2}+2\tau)} & \pm(2\tau,-3\tau,\tfrac{1}{2}) & \pm(-2,2+\tau,\tfrac{3}{2}+2\tau) & \pm(-1,1+2\tau,\tfrac{3}{2}+\tau) & \pm(-1-2\tau,1+2\tau,-\tfrac{1}{2}+\tau)
\end{array}
\tag{1.11}
$$

Ordering the A_2 orbits by their α_3 coordinate, we find that the upper half of C_{60} consisting of the orbits (identified by their dominant weights)

$$
\boxed{(1,1,\tfrac{3}{2}+3\tau)},\ \boxed{(2,\tau,\tfrac{3}{2}+2\tau)},\ \boxed{(2+\tau,0,\tfrac{1}{2}+2\tau)},\ \boxed{(1,2\tau,\tfrac{3}{2}+\tau)},\ \boxed{(1+\tau,0,-\tfrac{1}{2}+\tau)},\ \boxed{(\tau,2\tau,\tfrac{1}{2})},
$$

while in the lower half the dominant weights of the A_2 orbits of C_{60} have the sign of the third coordinate reversed, and the first two coordinates interchanged.

$$
\boxed{(2\tau,\tau,-\tfrac{1}{2})},\ \boxed{(0,1+\tau,\tfrac{1}{2}-\tau)},\ \boxed{(2\tau,1,-\tfrac{3}{2}-\tau)},\ \boxed{(0,2+\tau,-\tfrac{1}{2}-2\tau)},\ \boxed{(\tau,2,-\tfrac{3}{2}-2\tau)},\ \boxed{(1,1,-\tfrac{3}{2}-3\tau)},
$$

1.3.1. C_{60} as the stack of A_2 pancakes

Looking at C_{60} along the plane spanned by ω_1 and ω_2, the orbits of A_2 are viewed as horizontal segments, while the vertical direction is that of α_3. The structure is particularly visible in Fig. 1.2.

1.4. Symmetry breaking $C_{60} \to A_2$

Breaking the icosahedral symmetry H_3 to that of A_2 (dihedral group of order 6) is the main subject here. It is applied to the reduction of the icosahedral symmetry H_3 of C_{60} to the 12 orbits of A_2. The reduction yields eight hexagonal orbits of A_2 and four triangular ones.

There are five different polytopes with 78 C atoms forming 29 hexagons and 12 pentagons on their surfaces. In order to distinguish the five cases, we use the notation $C_{78}(I)$, $C_{78}(II)$, ..., $C_{78}(V)$, and these are shown in Figs. 1.3, 1.4, 1.6 and 1.7 respectively.

Breaking of the H_3 symmetry to its subgroup A_2, amounts to two operations: (i) insertion of several additional orbits of A_2 into the middle of the structure as in Fig. 1.2, and (ii) appropriate displacement of the upper and lower halves of C_{60} along the α_3-axis vector. The two operations are subject to the general requirement that the shell of the resulting polytope is formed as before by regular hexagons and 12 pentagons.

1.4.1. Polytopes $C_{78}(I)$ and $C_{78}(II)$.

Only the polytopes $C_{78}(I)$ (Fig. 1.3) and $C_{78}(II)$ (Fig. 1.4) occur as a result of the symmetry breaking $H_3 \to A_2$. They correspond to two possible variants of insertions of the middle belt into C_{60} (see Fig. 1.3 and 1.4). The two cases can be distinguished by looking at the pairs of nearest pentagons. In $C_{78}(I)$ they are linked by an edge of the polytope, while in $C_{78}(II)$ any two nearest pentagons are connected by a hexagon.

The middle belts of Fig. 1.3 and 1.4 display a mismatch between the vertices and edges of pentagons and of hexagons. The mismatch has a contribution from three different factors: (i) unwrapping the belt to a plane from the rounded C_{78}, (ii) the angles between edges within pentagons and/or hexagons can be distorted and (iii) the edges of the polytope may be bent and not of the same length. Only very precise measurement of real carbon polytopes may reveal how much each of these three factors contribute to the mismatch.

The central ring of nine hexagons in Fig. 1.3 and 1.4 can be extended to three hexagonal rings, forming C_{114}. Adjacent rings of six hexagons and three pentagons from both sides of the hexagon rings would fit the triple ring. Continuing further, one can build $C_{60+18(2k+1)}$ by inserting $2k+1$ hexagonal rings. At some k such extended polytopes should be considered as nanotubes.

When an even number of hexagonal rings is inserted as the middle ring, the lower (or upper) part of the original C_{60} polytope needs to be rotated by the angle $2\pi/18$ in order to match the lower (upper) part of the original polytope.

Polytope $C_{78}(II)$ and its analogs C_{96}, C_{114},..., and nanotubes arise in a similar way as in the case of $C_{78}(I)$. Additional rings of nine hexagons can be inserted into the middle of

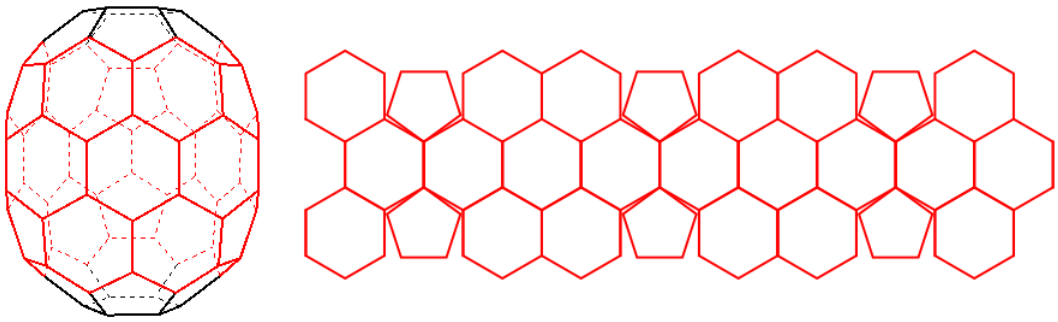

Figure 1.3. The $C_{78}(I)$ polytope together with its middle belt of the three rows of hexagons and pentagons unwrapped into the plane. Three pairs of vertically aligned pentagons that are linked by a hexagon-hexagon edge single out $C_{78}(I)$.

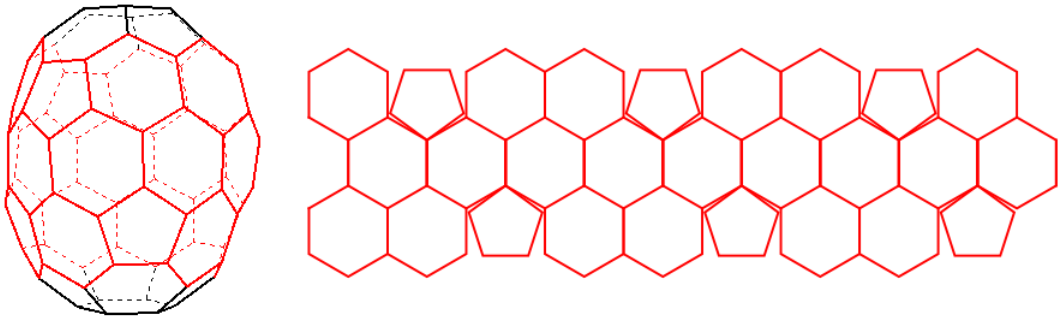

Figure 1.4. The $C_{78}(II)$ polytope together with its middle belt of the three rows of hexagons and pentagons unwrapped into the plane. Three pairs of pentagons linked by one hexagon single out $C_{78}(II)$.

$C_{78}(I)$ and $C_{78}(II)$, see Fig. 1.5. The greater is the number of hexagonal rings inserted, the longer the resulting nanotube that is built.

1.4.2. The polytope $C_{78}(III)$.

The polytope corresponding to $C_{78}(III)$ shown in Fig. 1.6 is also a result of symmetry breaking $H_3 \to A_2$, but is substantially different than $C_{78}(I)$ and $C_{78}(II)$. In those two cases (Fig. 1.3 and 1.4) the middle rings of the belts consist of nine hexagons aligned by their faces, while in $C_{78}(III)$ (Fig. 1.6) the middle ring consist of six pentagons, three hexagons and three edges. In fact $C_{78}(III)$ does not have a ring of nine hexagons oriented in any direction. Therefore it is not amenable to the formation of higher analogs of C_{78} and to nanotubes.

1.4.3. The polytopes $C_{78}(IV)$ and $C_{78}(V)$.

The polytopes $C_{78}(IV)$ and $C_{78}(V)$ in Fig. 1.7 can be viewed as combinations of $C_{78}(I)$ and $C_{78}(III)$. Indeed, in their middle belt one finds the formations pentagon-edge-pentagon oriented vertically, as in $C_{78}(I)$, as well as oriented horizontally, as in $C_{78}(III)$. Neither of

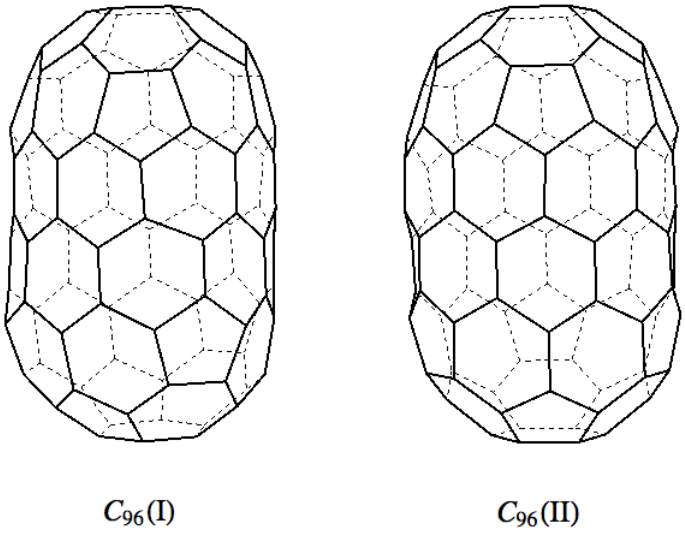

Figure 1.5. Two carbon structures C_{96} built from $C_{78}(I)$ and $C_{78}(II)$ by adding a ring of nine hexagons into the middle.

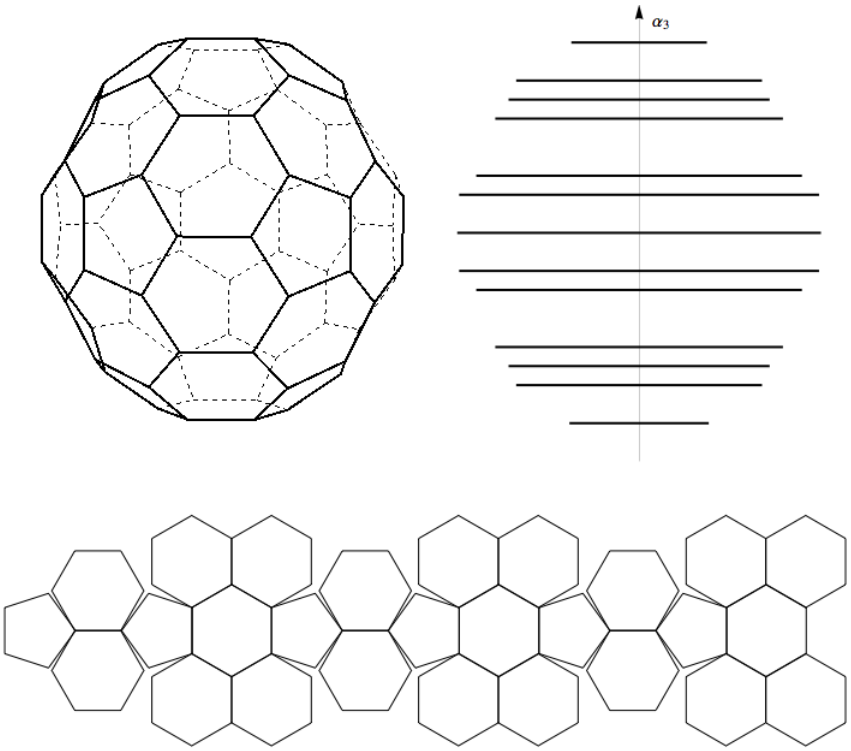

Figure 1.6. The polytope $C_{78}(III)$ together with its A_2-pancake structure and the middle belt of hexagons and pentagons unwrapped into the plane. Three pairs of horizontally aligned pentagons that are linked by a hexagon-hexagon edge single out $C_{78}(III)$.

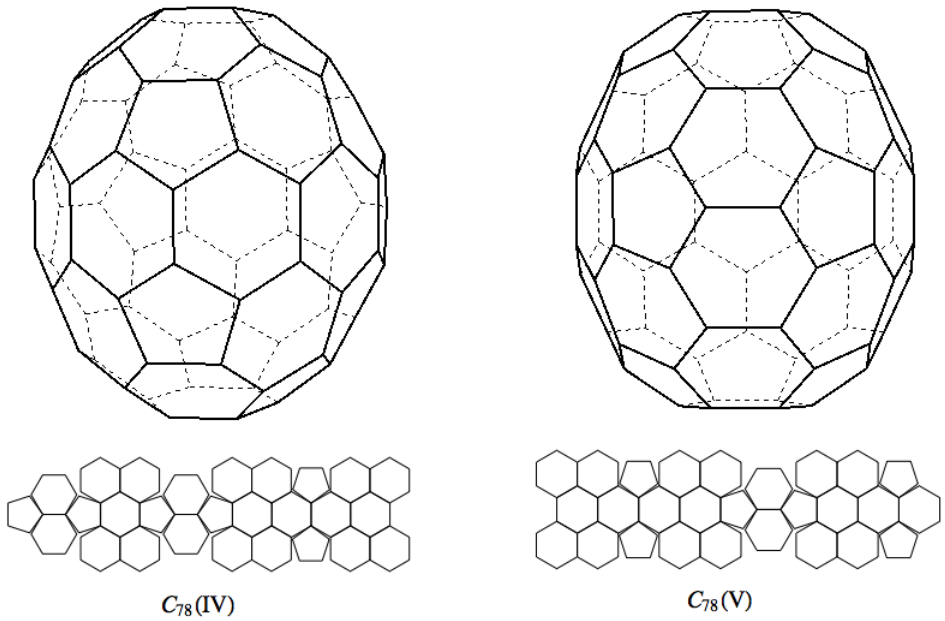

Figure 1.7. The polytopes $C_{78}(IV)$ and $C_{78}(V)$ and their middle belts of three rows of hexagons and pentagons unwrapped into the plane. Three pairs of pentagons that are linked by a hexagon-hexagon edge single out $C_{78}(IV)$, if two of the pairs are oriented horizontally and one vertically. $C_{78}(V)$ is singled out if two of the pentagon pairs are oriented vertically and the third pair is oriented horizontally.

the two polytopes can be augmented to higher analogs or to nanotubes by the insertion of additional rings of nine hexagons.

1.5. Concluding remarks

The existence of large carbon molecules such as C_{60} led to a search and subsequent discovery of a number of even larger molecules. Considering just the combinatorial possibilities for joining regular pentagons and hexagons on a convex surface, however, leads to a very large number of structures which could be identified (Schwerdtfeger et al. [29]). If in addition, though, certain symmetry properties are required to be respected, the number of possible structures is drastically reduced, producing particular higher carbon molecules in line with those observed in nature.

In the first paper of the series of which this work is a part (Bodner et al. [2]), the mechanisms for production of higher carbon molecular structures utilizing symmetry reduction to a maximal subgroup H_2 of H_3 was studied, namely $H_3 \to H_2$. In the present paper, we examined a second possibility, which is the symmetry reduction $H_3 \to A_2$. This reduction to A_2, however, is not unique as in the reduction to H_2, and there is more than one way to achieve it.

A third possibility for carrying out the symmetry reduction $H_3 \to A_1 \times A_1$ will be reported elsewhere. This case, like in the case of H_2 symmetry reduction, is unique but is achieved by different means than the insertion of additional belts of hexagons into the middle of the C_{60} surface.

Acknowledgements

The authors are grateful for the partial support of the work by the Natural Sciences and Engineering Research Council of Canada and by the MIND Research Institute in Irvine, California.
M.S. would like to express her gratitude to the Centre de recherches mathématiques, Université de Montréal, for the hospitality extended to her during her postdoctoral fellowship. She is also grateful to MITACS and OODA Technologies for partial support.

Chapitre 2

Icosahedral symmetry breaking : C_{60} to C_{84}, C_{108} and to related nanotubes

Cet article a été publié dans la revue *Acta Crystallographica Section A : Foundations and Advances* [voir 5].

Les principales contributions de *Emmanuel Bourret* à cet article sont présentées.

— découverte de la brisure de symétrie à appliquer et confirmation de cette hypothèse ;

— réalisation des calculs numériques générant les fullerènes ;

— aide à la rédaction de l'article ainsi qu'au processus de révision et de correction.

Icosahedral symmetry breaking : C_{60} to C_{84}, C_{108} and to related nanotubes

Mark Bodner
MIND Research Institute,
111 Academy Drive,
Irvine, CA, USA 92617

Emmanuel Bourret
Centre de recherches mathématiques,
Université de Montréal,
C.P. 6128, Succursale A,
Montréal, Canada H3C 3J7

Jiri Patera
Centre de recherches mathématiques,
Université de Montréal,
C.P. 6128, Succursale A,
Montréal, Canada H3C 3J7

Marzena Szajewska
Institute of Mathematics,
University of Bialystok,
1M Ciolkowskiego,
Bialystok, Poland PL-15-245

Résumé

Ce papier complète la série de trois articles indépendants [Bodner et al. [2, 4, 3]] décrivant la brisure de la symétrie icosaédrique en sous-groupes générés par réflexions dans l'espace euclidien tridimensionnel $\mathbb{R}^3$ comme mécanisme de génération de plus grands fullerènes à partir du C_{60}.

La symétrie icosaédrique du C_{60} peut être vue comme la jonction de 17 orbites d'un sous-groupe symétrique d'ordre 4 du groupe icosaédrique d'ordre 120. Ce sous-groupe est noté par $A_1 \times A_1$, car il est isomorphe au groupe de Weyl de l'algèbre de Lie semi-simple $A_1 \times A_1$. Treize des orbites de $A_1 \times A_1$ sont des rectangles et quatre sont des segments de droite. Les orbites forment un empilement de couches parallèles centrées sur l'axe du C_{60} passant par les centres de deux arêtes opposées entre deux hexagones sur la surface du C_{60}. Ces deux arêtes sont les deux seules couches de type segment de droite à apparaître sur la surface de la coquille.

Parmi les 24 polytopes convexes avec une coquille formée par des hexagones et 12 pentagones, ayant 84 sommets [Fowler and Manolopoulos [12, 13] ; Zhang et al. [33]], il y en a seulement deux qui peuvent être identifiés avec une brisure de la symétrie H_3 en $A_1 \times A_1$. Les autres ne sont que des coquilles convexes formées par des hexagones réguliers et 12 pentagones sans l'implication de la symétrie icosaédrique.

Mots-clés : groupe de Coxeter fini, brisure de symétrie, fullerènes, nanotubes

Abstract

This paper completes the series of three independent articles [Bodner et al. [2, 4, 3]] describing the breaking of icosahedral symmetry to subgroups generated by reflections in three-dimensional Euclidean space $\mathbb{R}^3$ as a mechanism of generating higher fullerenes from C_{60}.

The icosahedral symmetry of C_{60} can be seen as the junction of 17 orbits of a symmetric subgroup of order 4 of the icosahedral group of order 120. This subgroup is noted by $A_1 \times A_1$, because it is isomorphic to the Weyl group of the semisimple Lie algebra $A_1 \times A_1$. Thirteen of the $A_1 \times A_1$ orbits are rectangles and four are line segments. The orbits form a stack of parallel layers centered on the axis of C_{60} passing through the centers of two opposite edges between two hexagons on the surface of C_{60}. These two edges are the only two line segment layers to appear on the surface shell.

Among the 24 convex polytopes with shell formed by hexagons and 12 pentagons, having 84 vertices [Fowler and Manolopoulos [12, 13]; Zhang et al. [33]], there are only two that can be identified with breaking of the H_3 symmetry to $A_1 \times A_1$. The remaining ones are just convex shells formed by regular hexagons and 12 pentagons without the involvement of the icosahedral symmetry.

Keywords: finite Coxeter group, symmetry breaking, fullerenes, nanotubes

2.1. Introduction

In this paper, icosahedral symmetry and its implementation in the case of the fullerene C_{60} (see Fig. 2.1) is only briefly described, as its detailed exposition was presented in the two previous articles of the series (Bodner et al. [2, 4]) together with all notations.

The icosahedral group, denoted here by H_3, is of order 120. It is generated by three reflections, r_1, r_2, r_3 in the real Euclidean space $\mathbb{R}^3$. The simple roots α_1, α_2, and α_3 of H_3 are the normal vectors to the three reflection mirrors that meet at the origin and that define the icosahedral symmetry. They form the α-basis of the Euclidean space $\mathbb{R}^3$. A concise way to provide relative angles and a conventional choice of the lengths of the normals (Champagne et al. [9]), is to define the matrix C of their scalar products $\langle\alpha_j,\alpha_k\rangle$. In the case of H_3, one has,

$$C(H_3) = (\langle\alpha_j,\alpha_k\rangle) = \begin{pmatrix} 2 & -1 & 0 \\ -1 & 2 & -\tau \\ 0 & -\tau & 2 \end{pmatrix}, \qquad \tau = \tfrac{1}{2}(1+\sqrt{5})\,.$$

The ω-basis, reciprocal to α, is defined by

$$\langle\alpha_j,\omega_k\rangle = \delta_{jk}\,, \qquad j,k = 1,2,3\,. \tag{2.1}$$

Specifically we get the relations between the basis vectors,

$$\begin{aligned} &\alpha_1 = 2\omega_1 - \omega_2 && \omega_1 = (1+\tfrac{1}{2}\tau)\alpha_1 + (1+\tau)\alpha_2 + (\tfrac{1}{2}+\tau)\alpha_3 \\ &\alpha_2 = -\omega_1 + 2\omega_2 - \tau\omega_3 && \omega_2 = (1+\tau)\alpha_1 + (2+2\tau)\alpha_2 + (1+2\tau)\alpha_3 \\ &\alpha_3 = -\tau\omega_2 + 2\omega_3 && \omega_3 = (\tfrac{1}{2}+\tau)\alpha_1 + (1+2\tau)\alpha_2 + (\tfrac{3}{2}+\tfrac{3}{2}\tau)\alpha_3 \end{aligned} \tag{2.2}$$

In this paper, in addition to the α- and ω-bases, it is convenient to use the mixed basis $\{\omega_1,\alpha_2,\omega_3\}$ because according to equation (2.1), α_2 is orthogonal to the plane spanned by ω_1 and ω_3.

Suppose (a,b,c) is given relative to the basis $\{\omega_1,\omega_2,\omega_3\}$. In order to transform it to the basis $\{\omega_1,\alpha_2,\omega_3\}$, one proceeds as follows:

$$(a,b,c)\begin{pmatrix} 1 & 1+\tau & 0 \\ 0 & 2+2\tau & 0 \\ 0 & 1+2\tau & 1 \end{pmatrix} = (a,\, a+2b+c+(a+2b+2c)\tau,\, c)\,. \tag{2.3}$$

Thus one gets the following specific transformations:
$(1,1,0) \longrightarrow (1,3+3\tau,0)$, $\quad (0,-1-2\tau,3\tau) \longrightarrow (0,-1-\tau,-3\tau),\ldots$

The subgroup of interest to us here can be set up in H_3 in many equivalent ways. One of them is particularly transparent: two of the simple roots of H_3 that are orthogonal to each other can be adopted as the simple roots of $A_1 \times A_1$. Putting $\beta_1 = \alpha_1$ and $\beta_2 = \alpha_3$ we have

$$C(A_1 \times A_1) = (\langle\beta_p,\beta_q\rangle) = \left(\begin{smallmatrix} 2 & 0 \\ 0 & 2 \end{smallmatrix}\right), \qquad p,q = 1,2\,.$$

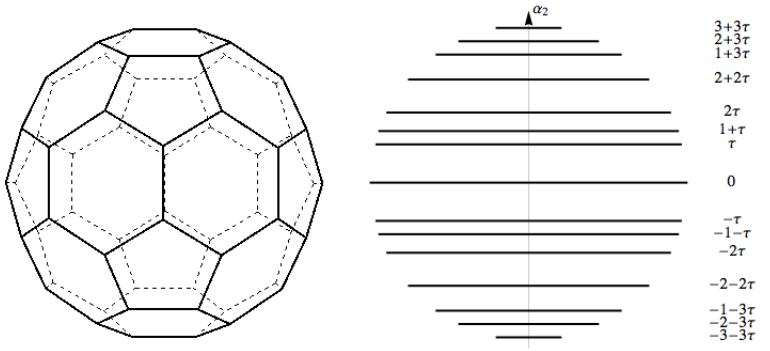

Figure 2.1. Two views of the polytope C_{60}. In one surface edges are shown. In the other only the orbits of $A_1 \times A_1$ are drawn as segments orthogonal to the axis of the polytope which is the simple root α_2. The last column of numbers contains coordinates of each $A_1 \times A_1$ orbit in the direction of α_2.

In the previous work we first considered the symmetry H_3 broken to the symmetry group H_2 that is generated by reflections r_2, r_3 (Bodner *et al.*, 2013), and second we considered the breaking of the H_3 symmetry to A_2, generated by the reflections r_1 and r_2 (Bodner et al. [4]). In the present paper the unbroken symmetry group is generated by the reflections r_1 and r_3. It is the Weyl group of the semisimple Lie group $SU(2) \times SU(2)$, or equivalently, of its semisimple Lie algebra $A_1 \times A_1$. The order of the group is 4. Hence its orbits consist of four, two or one point(s). It is convenient to write the orbit points in the ω-basis reciprocal to the α-basis of simple roots.

Reduction of the points of any orbit of H_3, in particular the 60 points/vertices of the polytope C_{60}, is found as in Bodner et al. [2, equation (11)]. In the list the vertices are given in the basis $\{\omega_1,\omega_2,\omega_3\}$. Only the dominant points that identify the orbits of the appropriate subgroup are pointed out.

2.2. The $A_1 \times A_1$ orbits of vertices of C_{60}

There are two images of C_{60} in Fig. 2.1. The first one is done traditionally by showing the edges of the surface of the polytope and their intersections (vertices). The second image shows only the $A_1 \times A_1$ orbits. Since the polytope is oriented vertically along the α_2 axis, the $A_1 \times A_1$ orbits appear as segments, thus forming the 'stack of pancakes', with each $A_1 \times A_1$ orbit being just one 'pancake'.

The $A_1 \times A_1$-orbit structure of C_{60} becomes visible once the dominant points of each orbit are identified, which is simplified by working in the ω-basis of $\mathbb{R}^3$. Indeed, it suffices to find among the 60 vertices those that have non-negative first and third coordinates in the ω-basis, indicating a non-action of the reflections r_1 and r_3 on the corresponding vertex/point. Each $A_1 \times A_1$ orbit has precisely one dominant point; therefore it is specified by it.

The 60 vertices of C_{60} are given below in pairs that differ by an overall sign. If the sign of the first and third coordinate of a vertex coincide, one of the pair is a dominant point of an $A_1 \times A_1$ orbit. Boxes mark all such pairs in equation (2.4). If both the first and the third coordinates are positive, the orbit contains four points. If one of the coordinates is 0, the orbit is a segment with two vertices at its extremes. The following 60 vertices of C_{60} are written in the basis $\{\omega_1,\alpha_2,\omega_3\}$. The formula (2.3) applied to the 60 vertices in ω-basis of Bodner et al. [2, equation (11)] results in the following points in the basis $\{\omega_1,\alpha_2,\omega_3\}$:

$$
\begin{array}{lll}
\boxed{\pm(1,3+3\tau,0)} & \boxed{\pm(2\tau,\tau,2+\tau)} & \boxed{\pm(1+2\tau,1+\tau,2)} \\
\pm(-2-\tau,2+2\tau,1) & \pm(2+\tau,2+2\tau,-1) & \boxed{\pm(-1,3+3\tau,0)} \\
\boxed{\pm(-1,1+3\tau,-2\tau)} & \boxed{\pm(2+\tau,2+2\tau,1)} & \pm(1,1+3\tau,-2\tau) \\
\pm(1+2\tau,1+\tau,-2) & \boxed{\pm(2,2+3\tau,\tau)} & \boxed{\pm(\tau,2\tau,1+2\tau)} \\
\boxed{\pm(-2\tau,\tau,-2-\tau)} & \pm(-1,1+3\tau,2\tau) & \pm(-2,2+3\tau,\tau) \\
\boxed{\pm(1,1+3\tau,2\tau)} & \boxed{\pm(-2,2+3\tau,-\tau)} & \boxed{\pm(-2-\tau,2+2\tau,-1)} \\
\pm(\tau,2\tau,-1-2\tau) & \pm(-2\tau,\tau,2+\tau) & \boxed{\pm(3\tau,0,1)} \\
\boxed{\pm(0,\tau,3\tau)} & \boxed{\pm(-\tau,2\tau,-1-2\tau)} & \pm(-1-2\tau,1+\tau,2) \\
\pm(2\tau,\tau,-2-\tau) & \boxed{\pm(0,\tau,-3\tau)} & \boxed{\pm(-1-2\tau,1+\tau,-2)} \\
\pm(-\tau,2\tau,1+2\tau) & \pm(3\tau,0,-1) & \pm(2,2+3\tau,-\tau)
\end{array}
\tag{2.4}
$$

Thus there are 13 rectangular orbits,

$$
\begin{array}{lll}
\boxed{(2\tau,\tau,2+\tau)} & \boxed{(1+2\tau,1+\tau,2)} & \boxed{(1,-1-3\tau,2\tau)} \\
\boxed{(\tau,-2\tau,1+2\tau)} & \boxed{(2,2+3\tau,\tau)} & \boxed{(2\tau,-\tau,2+\tau)} \\
\boxed{(1+2\tau,-1-\tau,2)} & \boxed{(1,1+3\tau,2\tau)} & \boxed{(\tau,2\tau,1+2\tau)} \\
\boxed{(2,-2-3\tau,\tau)} & \boxed{(2+\tau,-2-2\tau,1)} & \boxed{(2+\tau,2+2\tau,1)} \\
\boxed{(3\tau,0,1)} &&
\end{array}
\tag{2.5}
$$

and four orbits of two points,

$$
\boxed{(1,3+3\tau,0)} \quad \boxed{(1,-3-3\tau,0)} \quad \boxed{(0,\tau,3\tau)} \quad \boxed{(0,-\tau,3\tau)} \tag{2.6}
$$

Example 2.1.

The four orbits of 2 points:

$(1,1,0), r_1(1,1,0) = (-1,2,0)$, $\qquad (0,-1-2\tau,3\tau), r_3(0,-1-2\tau,3\tau) = (0,2+\tau,-3\tau)$.

$(1,-2,0), r_1(1,-2,0) = (-1,-1,0))$, $\qquad (0,-2-\tau,3\tau), r_3(0,-2-\tau,3\tau) = (0,1+2\tau,-3\tau)$.

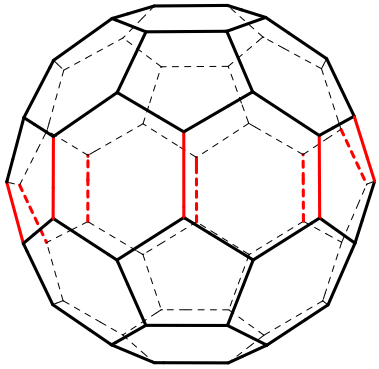

Figure 2.2. Coloured edges of C_{60} are to be removed before the insertion of additional spiral surface belts is undertaken. Removal of the edges also destroys four surface pentagons. They get replaced by four pentagons of the inserted spirals (Fig. 2.5).

Example 2.2.

Let us find the surface points of C_{60} *with the direction of the axis of* α_2 *which is orthogonal to the plane spanned by* ω_1 *and* ω_3*. Clearly the points* (1,1,0) *and* $r_1(1,1,0) = (-1,2,0)$ *are the end points of an edge on the top of* C_{60} *oriented as in Fig. 2.1. We have* $\alpha_2 \sim (1,1,0) + (-1,2,0) = (0,3,0)$.

Let us view C_{60} as the stack of $A_1 \times A_1$ pancakes. For that we look at the vertices of C_{60} in the direction parallel to the plane spanned by ω_1 and ω_3. Then each $A_1 \times A_1$ orbit appears as a segment. If in addition no edges on the surface of C_{60} are shown, we have the 'pancake stack' of C_{60} that is oriented in the direction orthogonal to the plane of ω_1 and ω_3, or equivalently, to vector α_2 (see Fig. 2.1).

Both images of C_{60} in Fig. 2.1 display exact icosahedral symmetry, so that no symmetry breaking has occurred.

2.3. Symmetry breaking $C_{60} \to A_1 \times A_1$

In the previous two papers of this series, related cases were considered of breaking the icosahedral symmetry of $C_{60} \to H_2$ (Bodner et al. [2]), and the symmetry breaking of C_{60} to A_2 (Bodner et al. [3]). These cases can also be described as choosing a subgroup generated by selecting two of the three reflections r_1, r_2, r_3 generating H_3.

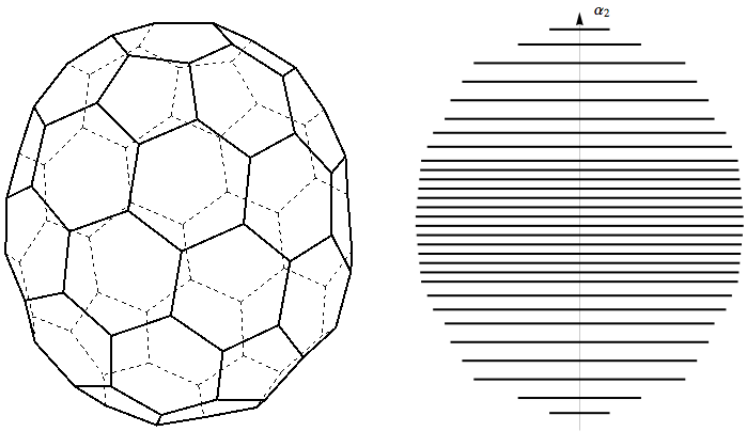

Figure 2.3. Pancake structure of C_{84}.

2.3.1. C_{84} from the $H_3 \to A_1 \times A_1$ symmetry breaking

The axis along which the symmetry breaking takes place in this paper is that of α_2. That is the reflections r_1 and r_3 remain as symmetry operations, while r_2 loses this role. The orbits of $A_1 \times A_1$ remain intact because they are in planes spanned by ω_1 and ω_3. In particular, the pancakes of Fig. 2.1 remain unchanged.

Symmetry breaking $C_{60} \longrightarrow A_1 \times A_1$ occurs in two steps:
(i) New orbits of $A_1 \times A_1$ are inserted into the C_{60} pancake stack.
(ii) Existing orbits of $A_1 \times A_1$ are displaced along the α_2 direction.

Both steps are subject to the additional constraint that the surface of the new polytope must be closed convex and formed by regular hexagons and 12 regular pentagons.

Both symmetry-breaking steps can be repeated any desired number of times.

Fig. 2.2 shows which edges of polytope have to be removed before the insertion of new orbits is undertaken.

2.3.2. Inserted spirals

It remains to describe the orbits of $A_1 \times A_1$ that should be inserted into the stack of C_{60} in Fig. 2.1 so that it becomes the stack of C_{84} in Fig. 2.3.

This cannot be achieved here by insertion of one or several rings of hexagons into a surface of C_{60} as was the case (Bodner et al. [2, 3]). Here symmetry breaking is taking place through the insertion of one or several spiral loops of hexagons. Since a spiral can be left- or right-hand oriented in $\mathbb{R}^3$, there are two versions for each new polytope. In Fig. 2.4 both versions of C_{84} are shown.

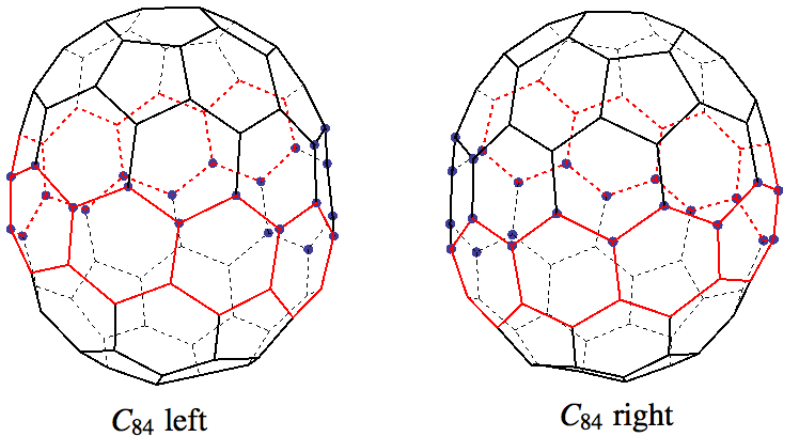

Figure 2.4. Left and right versions of C_{84} polytopes. The two versions differ by orientation of the inserted spiral belt with respect to the direction of α_2. Their pancake stacks coincide. Black circles indicate the 24 vertices that were added to C_{60}.

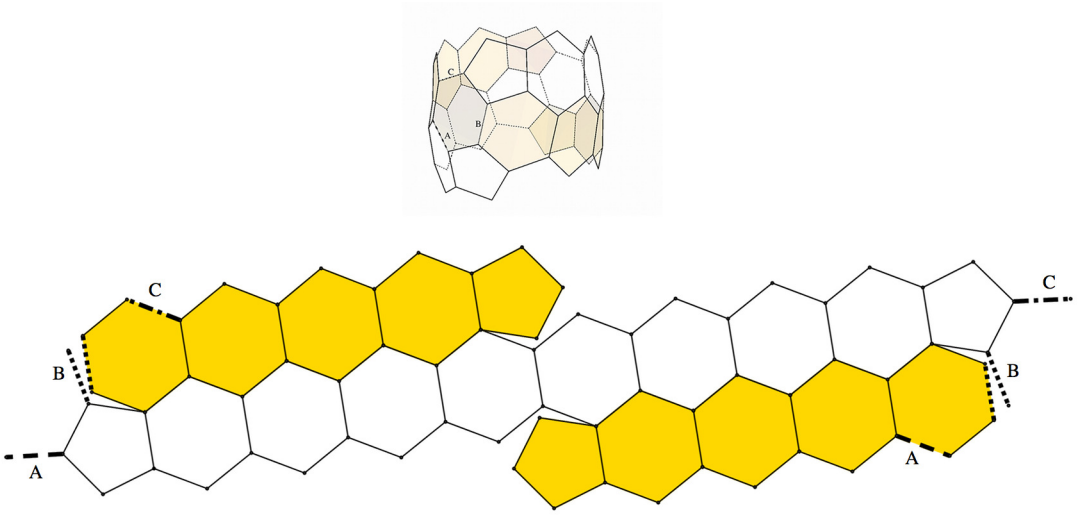

Figure 2.5. Flattened spiral that, added to C_{60}, transform it to C_{84} The three types of dashed lines indicate which edges are to be identified

A flattened image of a one-loop spiral of eight hexagons is shown in Fig. 2.5. The pentagons at its extremes are either incorporated into continuation of the loop, or are part of the original polytope before the insertion.

Left and right oriented spirals of polytopes C_{108}, C_{132}, ..., and nanotubes arise in a similar way as in the case of C_{84}. Each time the additional two rings of six hexagons (24 new vertices) can be inserted into the middle of the structure (see Fig. 2.6). The greater the number of pairs of hexagonal rings inserted, the longer the resulting nanotube that is built.

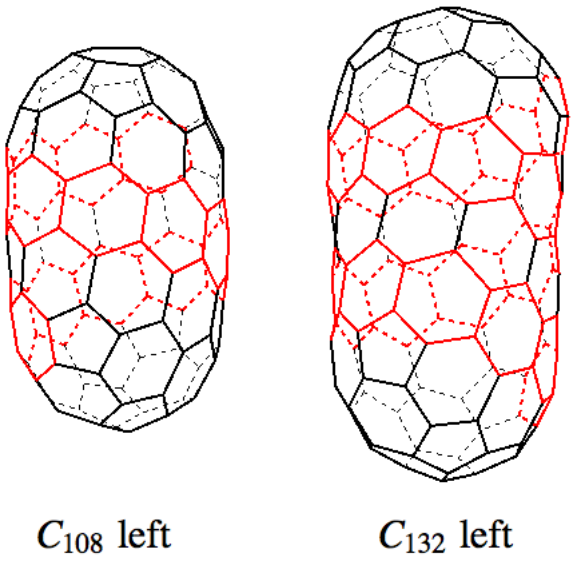

Figure 2.6. Left versions of the polytopes C_{108} and C_{132}, where multiple spiral belts (see Fig. 2.5) were added.

2.4. Concluding Remarks

Breaking of the icosahedral symmetry of C_{60} to the subgroup $A_1 \times A_1$ is the most complicated of the three possible methods of constructing nanotubes through the repeated application of the symmetry-breaking mechanism. Indeed, in Bodner et al. [2, 3] an appropriate number of rings of hexagons and pentagons was inserted between the upper and lower halves of the C_{60} shell.

One may be interested in constructing open-ended nanotubes rather than nanotubes that are closed on both ends; new versatile possibilities occur. Thus one can start from a single layer of graphene, which is the sheet of hexagons in $\mathbb{R}^2$. Then cutting a strip of constant width from the graphene, one can wrap it on a surface of a cylinder of an appropriate radius. It is important that both sides of the strip pass through identical sets of graphene points to have them matched seamlessly on the surface of the cylinder. Such a requirement still leaves an infinite (discrete) number of possible radii of the cylinder. The direction of the strip is dictated by the direction of the roots of the reflection groups.

Fullerenes and related nanotubes are sometimes used as carriers for other molecules in their interior. Symmetry alone admits several possibilities of defining special positions within fullerenes. A systematic description of such cases would be of interest.

An independent, interesting viewpoint on the structure of the fullerenes is found in Kostant [19, 20].

Acknowledgements

The authors are grateful for the partial support of the work by the Natural Sciences and Engineering Research Council of Canada and by the MIND Research Institute of Irvine, California.
M.S. would like to express her gratitude to the Centre de recherches mathématiques, Université de Montréal, for the hospitality extended to her during her postdoctoral fellowship. She is also grateful to MITACS for partial support.

Conclusion

Ce mémoire porte principalement sur la description de fullerènes et de nanotubes dont les symétries sont vues comme l'union d'orbites d'un sous-groupe symétrique du groupe icosaédrique d'ordre 120. L'approche utilisée est celle proposée par Bodner et al. [2, 4].

Deux chapitres composent le coeur de ce mémoire. Le premier décrit la brisure de symétrie du fullerène C_{60}, soit la symétrie du groupe H_3, par l'ajout d'orbites du sous-groupe A_2. L'ajout successif d'orbites permet l'obtention d'un nanotube de type zigzag. Le second répète essentiellement le même processus, mais en ajoutant cette fois des orbites du sous-groupe $A_1 \times A_1$, ce qui permet l'obtention d'un nanotube chiral.

La description de la brisure de symétrie icosaédrique pour les polytopes racinaires provenant du groupe non cristallographique H_3 a été présentée dans le cas où le polytope original est un icosaèdre tronqué (point dominant (1,1,0)), soit la représentation géométrique d'un fullerène C_{60}. Cependant, le groupe H_3 a deux autres orbites qui correspondent à des polytopes de 60 sommets ; le dodécaèdre tronqué et le rhombicosidodécaèdre dont les points dominants sont respectivement (0,1,1) et (1,0,1). La brisure de symétrie de ces deux polytopes similaires à des fullerènes et la construction des nanotubes résultants ne sont pas encore décrites et feront partie de mes sujets de recherche futurs en collaboration avec Z. Grabowiecka.

Une autre avenue de recherche intéressante serait d'utiliser une méthode similaire sur des fullerènes autres que le C_{60}. Étant donnée la nécessité de commencer avec une symétrie icosaédrique parfaite, il serait approprié de restreindre l'ensemble des potentiels candidats à ceux catégorisés dans le groupe I_h, selon la notation cristallographique de Schoenflies. Selon Gan [14], il n'y a que deux types de fullerènes avec un isomère I_h en terme de leurs propriétés géométriques. Le premier type comprend les fullerènes avec $20k^2$ sommets et le second ceux avec $60k^2$ sommets, où $k = 1,2,\ldots$. Ainsi, le fullerène C_{60} ne serait qu'un des cas les plus simples sur lequel appliquer la méthode. Un autre cas simple, dont les résultats préliminaires sont prometteurs, est celui du fullerène C_{20}, donc le diamètre est inférieur à celui du C_{60}. Cela laisse entrevoir qu'une telle généralisation du modèle permettrait de décrire des nanotubes de différents diamètres, à l'image de l'impressionnante variété de ces structures produites en laboratoire.

Un autre sujet qui nous intéresse est basé sur la description des vibrations des fullerènes. Une méthode a été décrite par Chadzitaskos et al. [8] pour quatre polytopes tridimensionnels provenant de quelques groupes cristallographiques, soit A_3, B_3, C_3, et un non cristallographique, H_3 qui est particulièrement intéressant pour nous. Les orbites de ces polytopes sont obtenues en utilisant le point dominant (1,1,1). Il serait potentiellement intéressant de décrire les vibrations pour le polytope associé au point dominant (1,1,0), soit celui associé au fullerène C_{60}, ou à d'autres polytopes similaires.

Bibliographie

[1] K. Balasubramanian. Topological characterization of five C_{78} fullerene isomers. *Chemical Physics Letters*, 206(1) :210 – 216, 1993. ISSN 0009-2614. doi : http://dx.doi.org/10.1016/0009-2614(93)85543-W. URL `http://www.sciencedirect.com/science/article/pii/000926149385543W`.

[2] M. Bodner, J. Patera, and M. Szajewska. C_{70}, C_{80}, C_{90} and carbon nanotubes by breaking of the icosahedral symmetry of C_{60}. *Acta Crystallographica Section A*, 69(6) : 583–591, Nov 2013. doi : 10.1107/S0108767313021375. URL `https://doi.org/10.1107/S0108767313021375`.

[3] M. Bodner, E. Bourret, J. Patera, and M. Szajewska. Icosahedral symmetry breaking : C_{60} to C_{78}, C_{96} and to related nanotubes. *Acta Crystallographica Section A*, 70(6) : 650–655, Nov 2014. doi : 10.1107/S2053273314017215. URL `https://doi.org/10.1107/S2053273314017215`.

[4] M. Bodner, J. Patera, and M. Szajewska. Breaking of icosahedral symmetry : C_{60} to C_{70}. *PLOS ONE*, 9(3) :1–5, 03 2014. doi : 10.1371/journal.pone.0084079. URL `https://doi.org/10.1371/journal.pone.0084079`.

[5] M. Bodner, E. Bourret, J. Patera, and M. Szajewska. Icosahedral symmetry breaking : C_{60} to C_{84}, C_{108} and to related nanotubes. *Acta Crystallographica Section A*, 71(3) : 297–300, May 2015. doi : 10.1107/S2053273315003824. URL `https://doi.org/10.1107/S2053273315003824`.

[6] N. Bourbaki. *Groupes et algèbres de Lie. Chapitres 4 à 6*. Bourbaki, Nicolas. Élements de mathematique. Springer, Berlin ; New York, 2007. ISBN 9783540344919.

[7] F. Cataldo, A. Graovac, and O. Ori. *Mathematics and topology of fullerenes*, volume 4 of *Carbon Materials : Chemistry and Physics*. Springer, 1 edition, 2011.

[8] G. Chadzitaskos, J. Patera, and M. Szajewska. Polytopes vibrations within coxeter group symmetries. *The European Physical Journal B*, 89(5) :132, May 2016. ISSN 1434-6036. doi : 10.1140/epjb/e2016-60891-2. URL `https://doi.org/10.1140/epjb/e2016-60891-2`.

[9] M. Champagne, B.and Kjiri, J. Patera, and R.T. Sharp. Description of reflection-generated polytopes using decorated coxeter diagrams. *Canadian Journal of Physics*,

73(9-10) :566–584, 1995. doi : 10.1139/p95-084. URL https://doi.org/10.1139/p95-084.

[10] L. Chen, R. V. Moody, and J. Patera. Non-crystallographic root systems in quasicrystals and discrete geometry. pages 135–178, 1998.

[11] M.S. Dresselhaus, G. Dresselhaus, and P.C. Eklund. *Science of Fullerenes and Carbon Nanotubes*. Academic Press, San Diego, 1996. ISBN 978-0-12-221820-0. URL http://www.sciencedirect.com/science/book/9780122218200.

[12] P.W. Fowler and D.E. Manolopoulos. Magic numbers and stable structures for fullerenes, fullerides and fullerenium ions. *Nature*, 355(6359) :428–430, Jan 30 1992. ISSN 0028-0836. doi : {10.1038/355428a0}.

[13] P.W. Fowler and D.E. Manolopoulos. *An Atlas of Fullerenes*. Dover Publications, 2007.

[14] L.H. Gan. Constructing ih symmetrical fullerenes from pentagons. *Journal of chemical education*, 85(3) :444, 2008.

[15] V. Georgakilas, J. A. Perman, J. Tucek, and R. Zboril. Broad family of carbon nanoallotropes : Classification, chemistry, and applications of fullerenes, carbon dots, nanotubes, graphene, nanodiamonds, and combined superstructures. *Chemical Reviews*, 115(11) :4744–4822, Jun 2015. ISSN 0009-2665. doi : 10.1021/cr500304f. URL https://doi.org/10.1021/cr500304f.

[16] P.J.F. Harris. *Carbon Nanotubes and Related Structures : New Materials for the Twenty-first Century*. Cambridge University Press, 1999. ISBN 9780521554466.

[17] J. E. Humphreys. *Introduction to Lie algebras and representation theory*. Graduate texts in mathematics, 9. Springer-Verlag, N.Y., 1972. ISBN 0387900527.

[18] J. E. Humphreys. *Reflection groups and coxeter groups*. Cambridge studies in advanced mathematics ; 29. Cambridge University Press, Cambridge England ; New York, 1st pbk. ed. (with corrections).. edition, 1992. ISBN 0521436133.

[19] B. Kostant. Structure of the truncated icosahedron (such as fullerene or viral coatings) and a 60-element conjugacy class in psl(2, 11). *Proc Natl Acad Sci USA*, 91(24) : 11714–11717, Nov 1994. ISSN 0027-8424. URL http://www.ncbi.nlm.nih.gov/pmc/articles/PMC45302/. 11607498[pmid].

[20] B. Kostant. The graph of the truncated icosahedron and the last letter of galois. *Notices of the American Mathematical Society*, 42, 09 1995. URL http://www.ams.org/notices/199509/kostant.pdf.

[21] Y. Lin, W. Cai, and X. Shao. Comparison studies of fullerenes C_{72}, C_{74}, C_{76} and C_{78} by tight-binding monte carlo and quantum chemical methods. *Journal of Molecular Structure : THEOCHEM*, 760(1) :153 – 158, 2006. ISSN 0166-1280. doi : http://dx.doi.org/10.1016/j.theochem.2005.12.006. URL http://www.sciencedirect.com/science/article/pii/S016612800500895X.

[22] Y.T. Lin, R.K. Mishra, and S.L. Lee. Capping C_{72} through C_6 : studying the relative stability of the five C_{78} fullerene isomers. *Chemical Physics Letters*, 302(1) :108 – 112, 1999. ISSN 0009-2614. doi : http://dx.doi.org/10.1016/S0009-2614(99)00063-9. URL http://www.sciencedirect.com/science/article/pii/S0009261499000639.

[23] R. V. Moody and J. Patera. Quasicrystals and icosians. *Journal of Physics A : Mathematical and General*, 26(12) :2829, 1993. URL http://stacks.iop.org/0305-4470/26/i=12/a=022.

[24] K. S. Novoselov, A. K. Geim, S. V. Morozov, D. Jiang, Y. Zhang, S. V. Dubonos, I. V. Grigorieva, and A. A. Firsov. Electric field effect in atomically thin carbon films. *Science*, 306(5696) :666–669, 2004. ISSN 0036-8075. doi : 10.1126/science.1102896. URL http://science.sciencemag.org/content/306/5696/666.

[25] K. S. Novoselov, V. I. Fal'ko, L. Colombo, P. R. Gellert, M. G. Schwab, and K. Kim. A roadmap for graphene. *Nature*, 490 :192 EP –, Oct 2012. URL http://dx.doi.org/10.1038/nature11458. Review Article.

[26] D. G. Papageorgiou, I. A. Kinloch, and R. J. Young. Mechanical properties of graphene and graphene-based nanocomposites. *Progress in Materials Science*, 90 :75 – 127, 2017. ISSN 0079-6425. doi : https://doi.org/10.1016/j.pmatsci.2017.07.004. URL http://www.sciencedirect.com/science/article/pii/S0079642517300968.

[27] P. Ramond. *Group Theory : A Physicist's Survey*. Cambridge University Press, 2010. ISBN 9781139489645.

[28] P. Schwerdtfeger, L. Wirz, and J. Avery. Program fullerene : A software package for constructing and analyzing structures of regular fullerenes. *Journal of Computational Chemistry*, 34(17) :1508–1526, 2013. ISSN 1096-987X. doi : 10.1002/jcc.23278. URL http://dx.doi.org/10.1002/jcc.23278.

[29] P. Schwerdtfeger, L. Wirz, and J. Avery. Program fullerene : A software package for constructing and analyzing structures of regular fullerenes. *Journal of Computational Chemistry*, 34(17) :1508–1526, 2013. ISSN 1096-987X. doi : 10.1002/jcc.23278. URL http://dx.doi.org/10.1002/jcc.23278.

[30] M. Szajewska. Faces of Platonic solids in all dimensions. *Acta Crystallographica Section A*, 70(4) :358–363, Jul 2014. doi : 10.1107/S205327331400638X. URL https://doi.org/10.1107/S205327331400638X.

[31] D. Wang, H. Shen, and Y. Zhai. Theoretical study on molecular electrostatic potential of C_{78}. *Journal of Rare Earths*, 25(2) :210 – 214, 2007. ISSN 1002-0721. doi : http://dx.doi.org/10.1016/S1002-0721(07)60075-1. URL http://www.sciencedirect.com/science/article/pii/S1002072107600751.

[32] Yujia Z., Zhen Z., and Hongwei Z. Graphene : Fundamental research and potential applications. *FlatChem*, 4 :20 – 32, 2017. ISSN 2452-2627. doi : https://doi.org/10.1016/j.flatc.2017.06.008. URL http://www.sciencedirect.com/science/article/

pii/S2452262717300508.

[33] B.L. Zhang, C.Z. Wang, K.M. Ho, C.H. Xu, and C.T. Chan. The geometry of large fullerene cages : C_{72} to C_{102}. *The Journal of Chemical Physics*, 98(4) :3095–3102, 1993. doi : 10.1063/1.464084. URL http://dx.doi.org/10.1063/1.464084.